

Research Article

Image Denoising Algorithm Using Second Generation Wavelet Transformation and Principle Component Analysis

Asem Khmag, Abd Rahman Ramli, S.A.R. Al-Haddad, S.J. Hashim and Zarina Mohd Noh
Department of Computer and Communication Systems, Faculty of Engineering, Universiti Putra
Malaysia, 43400, Serdang, Malaysia

Abstract: This study proposes novel image denoising algorithm using combination method. This method combines both Wavelet Based Denoising (WBD) and Principle Component Analysis (PCA) to increase the superiority of the observed image, subjectively and objectively. We exploit the important property of second generation WBD and PCA to increase the performance of our designed filter. One of the main advantages of the second generation wavelet transformation in noise reduction is its ability to keep the signal energy in small amount of coefficients in the wavelet domain. On the other hand, one of the main features of PCA is that the energy of the signal concentrates on a very few subclasses in PCA domain, while the noise's energy equally spreads over the entire signal; this characteristic helps us to isolate the noise perfectly. Our algorithm compares favorably against several state-of-the-art filtering systems algorithms, such as Contourlet soft thresholding, Scale mixture by WT, Sparse 3D transformation and Normal shrink. In addition, the combined algorithm achieves very competitive performance compared with the traditional algorithms, especially when it comes to investigating the problem of how to preserve the fine structure of the tested image and in terms of the computational complexity reduction as well.

Keywords: Cycle spinning, execution time, image quality, PSNR, wavelet based denoised

INTRODUCTION

Digital signals such as image, voice and video encounter many kinds of obstacles during transmission and acquisition. One of these troubles is the noises in different forms and types. Images are one of those digital signals that we are dealing with in many applications in our daily life, whether when we upload or download them with the World Wide Web applications or during scan usual documents, or even when we treat with medical images and so on. In order to be guaranteed that the images are free or less noise, we need to filter them using filtering system (denoising). Therefore, to build the filtering system in this study, there are two main points that is investigated in the literature. The first point is the Wavelet Based Denoising (WBD) and the other issue is the Principle Component Analysis (PCA).

Firstly, Wavelet based denoising algorithms have been used widely and effectively in digital image processing where those algorithms propose a perfect mathematical approach in order to deal with multire solution signals. The decorrelation, decreasing dimensionality, localization are considered as the most common characteristics of wavelet transformation. In addition, sparsity property is considered as the main feature of the second generation wavelet transform

where it maps the white noise in the signal class to white noise in the transform domain are also the main attributes of WT. Those attributes offer the advantage to execute the analysis approaches in the wavelet domain; instead of using it in the original domain (Abry *et al.*, 2002; Lio *et al.*, 2008; Asem *et al.*, 2014). Wavelet based denoising techniques are effectively used in several applications (Wink and Roerdink, 2004; Hesamoddin *et al.*, 2005; Gupta *et al.*, 2008) including parametric and nonparametric regression and probability density estimation (Donoho *et al.*, 1995; Donoho and Johnstone, 1998), signal processing and image processing (Starck *et al.*, 1998; Chan and Shen, 2005; Weeks, 2006; Yasmin *et al.*, 2012). Wavelet transform contains many wavelets basis (Percival and Walden, 2000) and it has wide applications that differs from each other, as a result, it may need a several types of wavelet basis to enhance the efficiency of this transformation. However, the main question in this case is how the selection of a wavelet basis will effect on the competence of WBD techniques. Goldstein *et al.* (2000) found that usage of second generation wavelets may lead to increase the incoherent portions in the length scale of the wavelet domain. The pivotal issue in their study was how to keep the satisfied properties of wavelets when we want to deal with 2D data; it simply

Corresponding Author: Asem Khmag, Department of Computer and Communication Systems, Faculty of Engineering, Universiti Putra Malaysia, 43400, Serdang, Malaysia

This work is licensed under a Creative Commons Attribution 4.0 International License (URL: <http://creativecommons.org/licenses/by/4.0/>).

uses time-frequency localization and fast algorithms to accomplish the denoising steps.

The answer of their query is to stop the use of the translation and dilation functions that is used in the first generation wavelet transformation anymore. In our study, the calculation in the wavelet part is totally based on a new technique, it is called the lifting structure and also known as (second wavelet transformation), more details about the mathematical model of this technique is given in Raanan (2009).

Secondly, principal component analysis is considered as one of the most common multivariate data and signal analysis methods (Gruber *et al.*, 2004). It transfers the correlated linearly data to un-correlated data in special domain, known also by feature space and it has many applications such as dimensional reduction in Gaussian signals and it is used in a whitening process of noisy images as well (Hyvarinen *et al.*, 2011). More details about PCA's applications can be found in Jolliffe (2004). PCA can be accomplished by using eigen value corrosion of the data that contain covariance matrix. The data that has the largest eigen values may have the main data details. We use this feature to separate the pure signal from the noisy components and it gives effective results in the denoising algorithm.

The wavelet transformation has combined with PCA tool, it is called multi-scale PCA technique (Bakshi, 1999) and it is mainly used for statistical application and in data classification too. It has been developed to be used in image and signal processing application and mainly in image enhancement and in order to deal with different kinds of noises. Despite the fact that wavelet transform has proven its ability in noise reduction (denoising) and image filtering; it still uses a static wavelet basis function to represent the image coefficients. Moreover, some images have too much no table and sharp structure patterns, which make the representation using one particular wavelet basis difficult task. As a result, the wavelet transformation will present different kinds of visual artifacts in the resulted outputs known by spurious blips. In order to conquer the drawbacks of this technique, wavelet based denoising using second generation wavelets has combined with PCA to accomplish the adaptive filter and to improve successfully the images that contaminated with AWGN.

Our main aim is to combine second-generation wavelets with PCA and exploit Semi-soft thresholding approach to differentiate the noisy coefficients from the original signal. In addition, we use cycle spinning technique in this study to improve the visual appearance of the reconstructed image, especially in the periodic texture, sharp and fine edges of the target image

WBD-PCA denoised algorithm: WBD-PCA technique shows competitive results as we will see later, whereas the main principle of this technique is

based on the facilities that provided by second generation wavelet transformation (Goldstein *et al.*, 2000) and the principle component analysis. The following sections present brief explanation of the main characteristics of both techniques.

Denoising using WT: Assume that the noise free image is represented in 2 Darray as x_{ij} , $i, j = 1, \dots, N$, where $N \times N$ is the image's size, so the corrupted image is modeled as:

$$y_{ij} = x_{ij} + n_{ij} \quad i, j = 1, \dots, N \quad (1)$$

y_{ij} is the noisy image, x_{ij} represents the noise free image and n_{ij} is Identically Independently Distributed (*iid*) as $N(0, \sigma^2)$ known as Gaussian white noise, where the noise level is σ . The main objective is to eliminate the noise from the original image as much as we can and also to find \hat{x}_{ij} that represents the estimation value of x_{ij} with minimum Mean Squared Error (MSE):

$$MSE(\hat{x}) = \frac{1}{N^2} \sum_{i,j=1}^N (\hat{x}_{i,j} - x_{i,j})^2 \quad (2)$$

The Wavelet approach can offer a nonlinear technique for the noisy signals to separate the noisy coefficients from the image and in order to make the separation procedure an easy and effective process. This separation is known as wavelet thresholding. The wavelet thresholding denoising is used to deal with additive Gaussian noise and it was found by Donoho *et al.* (1995). Regarding their research, the wavelet coefficient will set to be nil if its absolute value less than the specific value; otherwise, the coefficients will be kept unchanged. This is according to the hard way, or it will be changed based on the soft strategy. The hard threshold uses a preservation technique which can be done as follows:

$$d_{j,k}^{Hard} = \begin{cases} 0, & d_{j,k} < \lambda \\ d_{j,k}, & d_{j,k} \geq \lambda \end{cases} \quad (3)$$

where, $d_{j,k}$ is as the coefficients in wavelet domain and (j, k) is the coordinate position of the coefficients and λ represents the threshold value.

This technique is mainly depending on the concept of the signal's energy and it can be characterized with only few numbers of chosen subsets from the coefficients which are designed to be untouched, while the noise is represented by some coefficients that normally spread in small values nearby zero value. It has too small values, which set up to be zero. Unfortunately, this method has shortcomings; where the patterns inside the image that closes to the edges texture, mainly tends to be blended with the noise. By applying the threshold filtering on these coefficients with hard technique, it will lead to wave oscillations close to the borders in the resulted image. By other meaning, it will cause the Gibbs phenomenon. Donoho

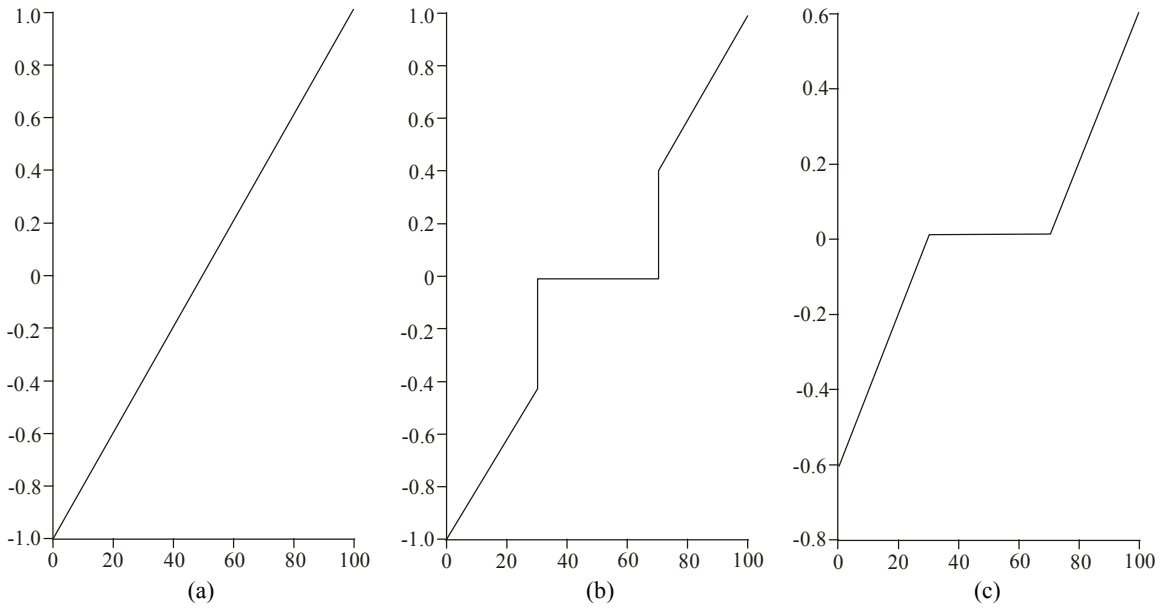


Fig. 1: (a) Original signal, (b) hard, (c) soft thresholding at $\sigma = 0.4$

and Johnstone (1998) indicated that the visual artifacts that resulted from the hard thresholding, it can be slightly revoked by using a different kind of thresholding technique; this technique is called soft thresholding. The main difference from the hard method lies on that, the soft technique modified the coefficients by the threshold λ , it can be done as the follows:

$$d_{j,k}^{soft} = sign(d_{j,k})(|d_{j,k}| - \lambda) \quad (4)$$

Figure 1 shows the original signal and the both techniques hard and soft.

Naturally, the hard thresholding technique tends to be more sensible. However, it sounds to present an unwanted visual artifact that affects the resulted outputs. Therefore, new method based on semi-soft thresholding will be proposed in this study.

This method overcomes the drawbacks in both types of thresholding technique (hard and soft), like killing too many coefficients and also discontinuity feature in hard thresholding and the over smoothing that affects the reconstructed image in soft type.

PCA based denoising: In this study, an effective principle component analysis based denoising algorithm will be presented. It is done by converting the noise free image dataset into PCA domain. This transformation will lead to keep just the best significant principal components, whereas, it was supposed to minimize the noisy components. However, PCA is a conventional technique to achieve the de-correlated dataset that can be widely used for dimensionality

reduction in several kinds of applications such as data compression, pattern recognition to further its wide range application in noise reduction (Muresan and Parks, 2003; Suganthy and Ramamoorthy, 2012). This easily can be done by:

$$X = \begin{bmatrix} x_1^1 x_1^2 \dots x_1^n \\ x_2^1 x_2^2 \dots x_2^n \\ \vdots \vdots \vdots \vdots \\ x_m^1 x_m^2 \dots x_m^n \end{bmatrix} \quad (5)$$

The model array of X , where $x_i^j, j = 1, 2, \dots, n$, are known as the discrete samples of variable $x_i, i = 1, 2, \dots, m$. The i^{th} row of sample array X , is indicated by:

$$x_i = [x_i^1 x_i^2 \dots x_i^n] \quad (6)$$

It is called the sample's vector of x_i . The mean value of x_i can be calculated as:

$$\mu_i = \frac{1}{n} \sum_{j=1}^n x_i(j) \quad (7)$$

Then the model vector x_i is computed as:

$$\bar{x}_i = x_i - \mu_i = [x_i^1 x_i^2 \dots x_i^n] \quad (8)$$

where, $\bar{x}_i^j = x_i^j - \mu_i$. Accordingly, the mean matrix of X is:

$$\bar{X} = [x_1^T x_2^T \dots x_M^T]^T \quad (9)$$

Finally, we can find out the co-variance matrix of the mean data model by:

$$\Omega = \frac{1}{N} \bar{X} \bar{X}^T \quad (10)$$

The main objective of PCA is to find out an orthonormal model of the matrix P in order to de-correlate \bar{X} , i.e., $\bar{Y} = P\bar{X}$. From this point we can proof that the co-variance matrix of \bar{Y} is diagonal. As the co-variance matrix Ω is symmetrical, so it is true to write it in the following form:

$$\Omega = \phi \Lambda \phi^T \quad (11)$$

Since $\phi = [\phi_1 \phi_2 \dots \phi_m]$ is the $m \times m$ orthonormal eigenvector array and $\Lambda = [\lambda_1 \lambda_2 \dots \lambda_m]$ is considered as diagonal eigenvalue matrix with $\lambda_1 \geq \lambda_2 \geq \dots \geq \lambda_m$ the term $\phi_1, \phi_2, \dots, \phi_m$ and $\lambda_1, \lambda_2, \dots, \lambda_m$ are represented by the eigenvectors and eigen values of Ω respectively, then by setting:

$$P = \phi^T \quad (12)$$

Then the sample \bar{X} can be de-correlated, i.e., $\bar{Y} = P\bar{X}$ and $\Lambda = \frac{1}{N} \bar{Y} \bar{Y}^T$.

METHODOLOGY

In this study, firstly, the noisy image is pre-filtered in order to get a better protection of the image small details and arrange it to be in the suitable mode to be filtered by WBD-PCA processes. The next step is to apply PCA transformation on the image in order to collect de-correlated datasets as in (1). It keeps the image structure when their coefficients get shrunk during the transformation in PCA in order to eliminate the artifacts. Thus, the denoised algorithm based on second generation wavelets is applied on the resulted image; the coefficients were divided into two fields, low and high frequency bands. Then the WBD using semi-soft thresholding will applied on the high frequency band regardless of the cross-correlations coefficients among the digital signals. Then, the resulted coefficients are returned to the original format by applying Inverse Wavelet (ISWT). The last step is to apply the cycle spinning on the reconstructed image in order to improve the high frequency component,

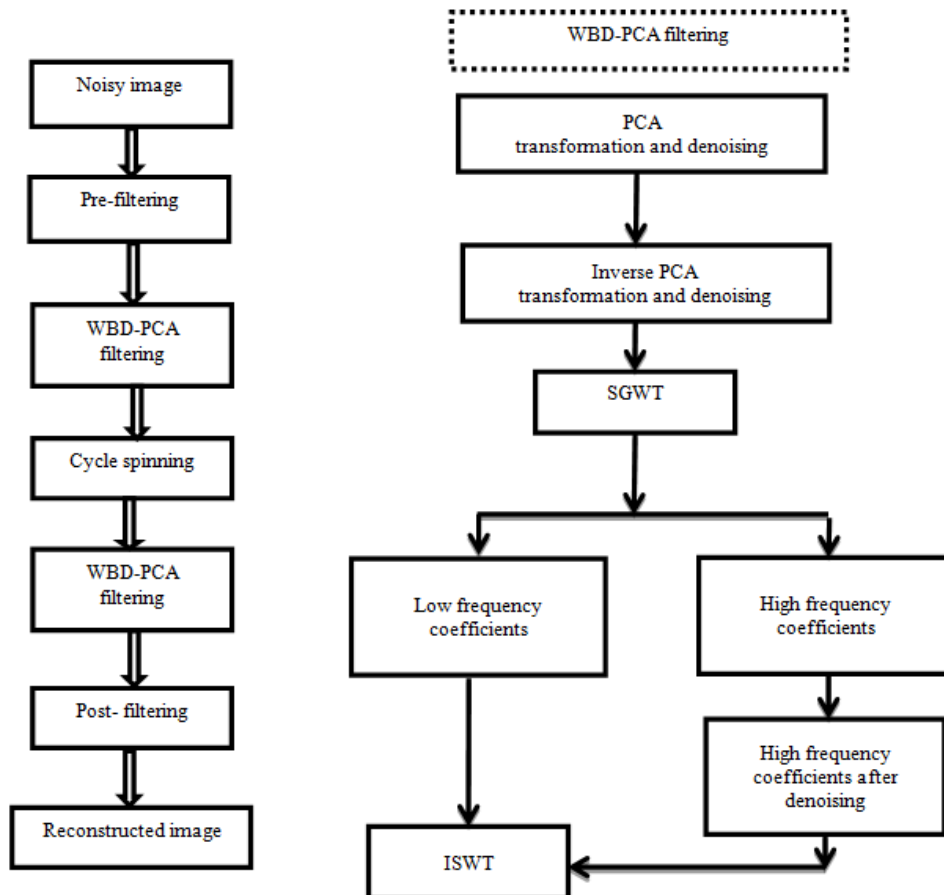


Fig. 2: The block diagram of WBD-PCA filter

especially on the textures that are near to the sharp edges. This technique is mostly experienced stunning results in order to remove the stationary noise as we will see in the experimental results, where PCA and WBD denoising procedure is applied to the contaminated image. The main steps of the proposed method are shown in Fig. 2.

Principle Component Analysis (PCA): The first step in the WBD-PCA filtering technique that is coming after the pre-filtering process is to apply PCA. PCA offers a competent procedure to remove the noise from the images during denoising processes, where the threshold value will be calculated with the noise's energy instead of calculating the variance of the noise that we will apply in the next step using WBD technique. Conventional PCA has the ability to resize the Contourlet details of the frequency sub bands that contains more details of the signal into only one vector dimensional that contains the eigenvectors of the tested image, then the covariance matrix will be calculated as it is discussed in Eq. (6) to (10). When we apply PCA on the noisy image, we will get de-correlated dataset \bar{Y} . The de-correlated dataset \bar{Y} represents the characteristics of the original dataset (noisy image). In this step the image is ready to be in wavelet format (de-correlated dataset) in order to apply the denoised based on second generation wavelet transformation.

Wavelet thersholding using semi-soft procedure: Wavelet coefficients are considered as correlated dataset and it is correlated in a few groups of the neighborhood. The great wavelet coefficients will possibly have great coefficients within the same region as well. Thus, the proposed thresholding approach can be derived from the neighborhood coefficients of the noisy image. Assume $B_{i,j}$ is the set of wavelet coefficients of the tested noisy image. Let:

$$U^2_{i,j} = \frac{B^2_{i,j-1} + B^2_{i,j} + B^2_{i,j+1}}{3} \quad (13)$$

where, $U^2_{i,j}$ is resulted from summation of square of the coefficients that its located in the same row of the coefficient under thresholding, (i, j) represents the coefficient location of the noisy image:

$$\text{if } U^2_{i,j} \geq \lambda^2 \quad (14)$$

Then the wavelet coefficients $B_{i,j}$ is set to zero. Otherwise, we shrink it according to:

$$B_{i,j} = \frac{B^2_{i,j} - \lambda^2 B^2_{i,j}}{U^2_{i,j}} \quad (15)$$

And $\lambda = \sqrt{2 \ln M_j} \times \sigma_w$, σ_w is the standard deviation of the noisy image, M_j represents the number of

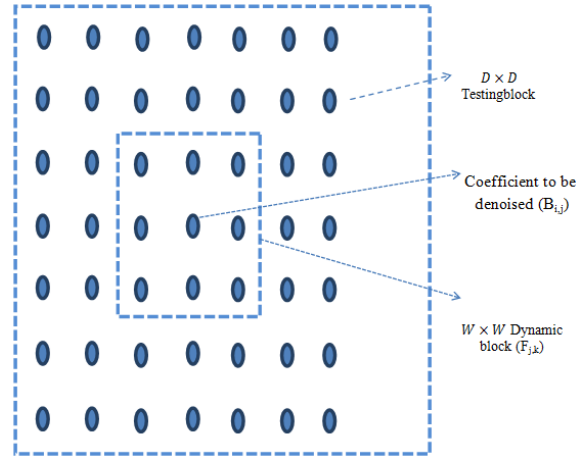


Fig. 3: The testing and dynamic block neighbourhood window that is located at the wavelet value to be shrunk

coefficients in a sub-band under consideration at the decomposition level j .

For every wavelet coefficient $B_{i,j}$ that is considered to be threshold, a square neighborhood window $D \times D$ represents the size of sub-block of the noisy image, this block is called testing block. In our experiments, the testing block is chosen to be 7×7 . Another square window is called Dynamic block $F_{j,k}$ is considered around the coefficient $B_{i,j}$ in order to apply the semi-soft thresholding. This means the size of the window in the neighbourhood is done as $W \times W$, where W is a positive odd number. W is chosen to be 3 in our experiments.

Figure 3 illustrates a 3×3 dynamic block window that is located at the wavelet quantity that needs to be shrunk and a window with 7×7 represents the testing block of the noisy image. Dividing the noisy image into testing blocks helps the thresholding process to be simple and uncomplicated. On the other hand, wavelet coefficient sub-bands should be individually threshold, where the borders of several sub-bands have de-correlated sort. Inverse second wavelet transformation is applied on the data matrix that is obtained after thresholding. In order to complete the denosing procedure, cycle spinning process is performed to increase the visual appearance of the reconstructed image.

Cycle spinning approach: The idea of using “cycle spinning” has been proposed in order to minimize the pseudo-Gibbs phenomena that may affect the resulted image, where it often exists in wavelet-based image reconstruction and denoising (Mohsen, 2004). This can be achieved as follows.

In the range of S shifts of the wavelet coefficients, there are a number of shifts that can be done on the image with size $M \times M$, horizontally or vertically or in both directions, then we perform denoising process on the shifted data using WBD technique and then un-shifts the denoised image in reverse manner. Doing

these shifts for each range of the image and take the average of the different results that come after the denoised steps. By applying the cycle spinning approach, we can produce a reconstruction subject to weaker pseudo-Gibbs phenomena that resulted from the denoising by using the second generation wavelet transforms.

Since the image is assumed to be in periodic pattern format with period M , better results can be obtained by using a higher number of shifts $S \in \{0, 1, 2, \dots, M-1\}$. When $S = M-1$, it is called total-shift cycle spinning. Otherwise, only partial shift cycle spinning is performed. Moreover, the quality of the denoised image, as measured by the subjective fidelity measures, improves extensively for the first few values of S -shifts. However, for larger value of S , there is no visible advantage that can be achieved by increasing S even further. In our experiments S is chosen to be 8. Thus, the cycle spinning approach may lead to increase the computation operations. Indeed, when incorporating this algorithm with S -shifts for any denoising method, the computational complexity is multiplied by S times.

Metric and proposed method quality assessment:

The definition of image quality came from the measures of the feature's image that has a kind of degradation characteristics and from this measurement we can classify the image whether it has good quality or not. There are several kinds of measures, Mean Squared Error (MSE), Peak Signal to Noise Ratio (PSNR), Structural Similarity Index (SSIM) and perceptual quality of human point of view were used to measure the efficiency of the projected technique (Wang *et al.*, 2004). The MSE and the PSNR show how physically the degraded image closed to the original image. However, they are not always correlated well with perceived picture quality.

Mean squared error carries the most significance as far as noise suppression is concerned. Let I be the original image, K -denoised image, i -pixel row index, j -pixel column index:

$$MSE = \frac{1}{m \cdot n} \sum_{i=0}^{m-1} \sum_{j=0}^{n-1} [I(i, j) - K(i, j)]^2 \quad (16)$$

Peak signal to noise ratio is measured in decibels (dB). In addition, it is scaled in the criteria of bits per trial or sample or it can be considered as bits per pixel scale. For example, if the tested image has 8 bits/pixel, it can be represented with pixel scale from 0 to 255. Greater PSNR value reflects better image quality and noise suppression:

$$PSNR = 10 \cdot \log_{10} \left(\frac{MAX^2}{MSE} \right) \quad (17)$$

Structural similarity index reflects the perceptual of the image class. It is based on the local structural details. It is considered as an objective image quality metric and it has an advantage among the traditional

measures like MSE and PSNR. In addition, the SSIM is a technique to measure the propinquity among signals and images. Further, it can be noticed as an excellence scale of any kind of images whether they are natural, MRI, or even Satellite images (Wang *et al.*, 2004):

$$SSIM(x, y) = [l(x, y)]^\alpha [c(x, y)]^\beta [s(x, y)]^\gamma \quad (18)$$

It is important to notice that $\alpha > 0$, $\beta > 0$ and $\gamma > 0$, those factors are used to prioritize the components:

$$l(x, y) = \frac{2\mu_x\mu_y + c_1}{2\mu_x^2 + 2\mu_y^2 + c_1} \quad (19)$$

$$c(x, y) = \frac{2\sigma_x\sigma_y + c_2}{2\sigma_x^2 + 2\sigma_y^2 + c_2} \quad (20)$$

$$s(x, y) = \frac{\sigma_{xy} + c_3}{\sigma_x\sigma_y + c_3} \quad (21)$$

$\mu_x = \sum_{i=1}^N w_i x_i$, μ_x represents the mean of the original image

$\sigma_x = \left(\sum_{i=1}^N w_i (x_i - \mu_x)^2 \right)^{\frac{1}{2}}$, σ_x represents the standard deviation of the reference image

$\sigma_{xy} = \sum_{i=1}^N w_i (x_i - \mu_x)(y_i - \mu_y)$, σ_{xy} represents the cross standard deviation amongst the noise free image and the noisy one

w = The circular symmetric Gaussian weighting function

c_1, c_2, c_3 = The three constant to prevent instability

RESULTS AND DISCUSSION

Natural images often contain many unrelated objects, thus they will make the image denoising technique a very tough task. We have applied the second generation wavelet transformation that combined with PCA in small image patches in the neighborhood frame with standard size that required for local denoising to many standard test images, including, Peppers, Lena, Tower and Parrot.

The size of the test images was 256×256. We applied the second generation WBD-PCA on all images, where the experiments on the noisy images with additive white Gaussian noise of $\sigma = 10, 20, 30$ and 40 were conducted. We choose the 3×3 dynamic block size and the size of training coefficients is chosen to be 7×7. The other parameter in our experiments was the number of spinning shifts in cycle spinning S , it is important to increase the quality appearance of the reconstructed image especially the areas near to the edges and high frequency components. In our experimental the number of S shifts is chosen to be 8.

Table 1 shows PSNR and SSIM of different standard images that have different noise levels (σ is

Table 1: PSNR and SSIM of the denoised images using different algorithms and at different standard deviation

| Algorithms | Contourlet soft thresholding | Scale mixture using wavelet transformation | Sparse-3D transformation | Normal shrink | WBD-PCA |
|---------------|------------------------------|--|--------------------------|---------------|---------------|
| Peppers | | | | | |
| $\sigma = 10$ | 31.5 (0.8660) | 33.3 (0.8901) | 33.6 (0.8939) | 33.3 (0.8777) | 34.7 (0.9008) |
| $\sigma = 20$ | 28.5 (0.8009) | 30.1 (0.8381) | 30.6 (0.8496) | 29.9 (0.8301) | 31.2 (0.8564) |
| $\sigma = 30$ | 26.6 (0.7880) | 28.3 (0.7968) | 28.8 (0.8108) | 28.2 (0.7901) | 29.2 (0.8211) |
| $\sigma = 40$ | 25.9 (0.7223) | 26.9 (0.7552) | 27.2 (0.7729) | 26.9 (0.7622) | 27.7 (0.7896) |
| Lena | | | | | |
| $\sigma = 10$ | 32.4 (0.8776) | 33.2 (0.9160) | 33.9 (0.9272) | 33.5 (0.8889) | 35.2 (0.9377) |
| $\sigma = 20$ | 29.1 (0.7909) | 29.4 (0.8514) | 30.2 (0.8699) | 30.0 (0.8311) | 31.6 (0.8902) |
| $\sigma = 30$ | 27.1 (0.7544) | 27.5 (0.7964) | 28.3 (0.8231) | 28.5 (0.8002) | 29.6 (0.8409) |
| $\sigma = 40$ | 25.8 (0.7115) | 26.0 (0.7466) | 27.3 (0.7727) | 27.1 (0.7433) | 28.3 (0.7999) |
| Tower | | | | | |
| $\sigma = 10$ | 32.4 (0.8975) | 34.8 (0.9079) | 35.0 (0.9144) | 34.7 (0.9112) | 35.5 (0.9200) |
| $\sigma = 20$ | 30.2 (0.8399) | 31.1 (0.8444) | 31.6 (0.8576) | 31.2 (0.8511) | 32.1 (0.8642) |
| $\sigma = 30$ | 28.2 (0.7804) | 29.2 (0.7919) | 29.7 (0.8135) | 29.5 (0.8098) | 30.3 (0.8309) |
| $\sigma = 40$ | 26.7 (0.7433) | 27.9 (0.7505) | 28.3 (0.7760) | 28.1 (0.7566) | 29.0 (0.7866) |
| Parrot | | | | | |
| $\sigma = 10$ | 32.7 (0.8998) | 34.1 (0.9190) | 34.6 (0.9274) | 34.3 (0.9210) | 35.6 (0.9303) |
| $\sigma = 20$ | 30.0 (0.8344) | 30.6 (0.8665) | 31.2 (0.8832) | 30.8 (0.8772) | 32.3 (0.8899) |
| $\sigma = 30$ | 28.2 (0.8201) | 28.6 (0.8269) | 29.3 (0.8505) | 28.9 (0.8333) | 30.2 (0.8801) |
| $\sigma = 40$ | 26.4 (0.7112) | 27.2 (0.7925) | 27.5 (0.8175) | 27.0 (0.7687) | 28.6 (0.8565) |

The value in parenthesis represent the SSIM measurement

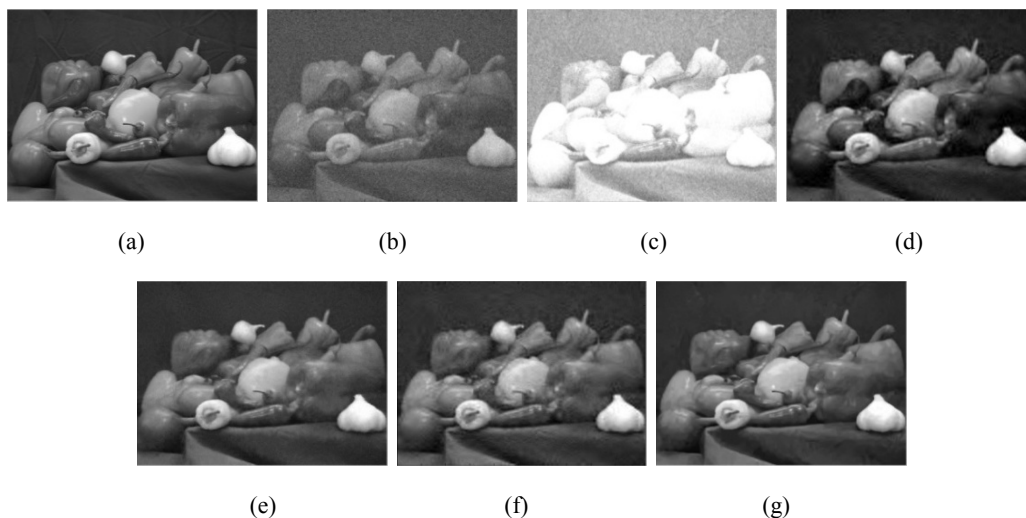


Fig. 4: The denoised images results of peppers by different schemes, (a) noisy-free, (b) noisy with $\sigma = 20$, (c-g) are denoised images by using: by contourlet soft, scale mixture using WT, sparse 3D transformation, normal shrink and the suggested algorithm, respectively

scaled between 10 to 40). In this table, different images compared with most common traditional algorithms in the denoising field. The proposed algorithm has the highest PSNR and outperformed the standard algorithm by (3.2 to 1.1 dB) in Peppers and (2.8 to 1.2 dB) in Lena and (3.1 to 0.8 dB) in Tower and finally (2.7 to 1 dB) in Parrot. It is clear to notice that the values of SSIM for different images in Table 1, is written in brackets; the higher SSIM was in the proposed algorithm with 0.9377 in Lena. On the other hand, images with high texture details such as Parrot and Tower had the lowest SSIM. It is because of the rich amount of image details in the original images. The value of SSIM decreases whenever the amount of noise level σ increases, it experienced the lowest value in Lena image with noise level at $\sigma = 40$.

Figure 4 to 7 shows the denoised images (Lena, Peppers, Parrot and Tower) that resulted from the four contaminated images, where the noise level $\sigma = 20$ is chosen in the figures using different algorithms. The sub-figure (a) represents the free noise image; (b) is a noisy image, the sub-figures (c-g) are the denoised images by Contourlet soft, Scale mixture using WT, Sparse 3D transformation, Normal shrink and the suggested WBD-PCA algorithm, respectively. In spite the sparse 3D transformation has the closest SSIM measures to our algorithm, still its appearance has visually blurred. The images that are reconstructed using Contourlet soft thresholding seem to have more brightness compared with the images achieved with other techniques and this is because of the abrupt change in the pixel values. The images that reconstructed by the Scale mixture using WT denoising

method has the worst visual quality. The justification behind this appearance is because in wavelet thresholding technique similar wavelet basis function that has the same dilation and translation is used to decorrelate the details of the image. The images that achieved by Normal shrink algorithm has blurred characteristic, despite it having higher SSIM. By other words, objectively they seem to be unclear especially in regions near to the edges and in flat zones as well. The proposed method using second generation WBD-PCA has very clear visual quality, it gets this benefit from

the characteristics of the second wavelet transformation that combined with PCA to reduce the dimensionality and separate the noise from energy coefficients. It has the highest visual quality compared to the other algorithms. To summarize, it is clear to say that the proposed algorithm WBD-PCA has the best visual quality and also in terms of PSNR and SSIM. In addition, the sparse 3D transformation has an acceptable visual as well, but in terms of execution time it takes a long time before the results can be ready as it will be mentioned later.



Fig. 5: The denoised images results of Lena by different schemes, (a) noisy-free, (b) noisy with $\sigma = 20$, (c-g) are denoised images by using: by contourlet soft, scale mixture using WT, sparse 3D transformation, normal shrink and the suggested algorithm, respectively

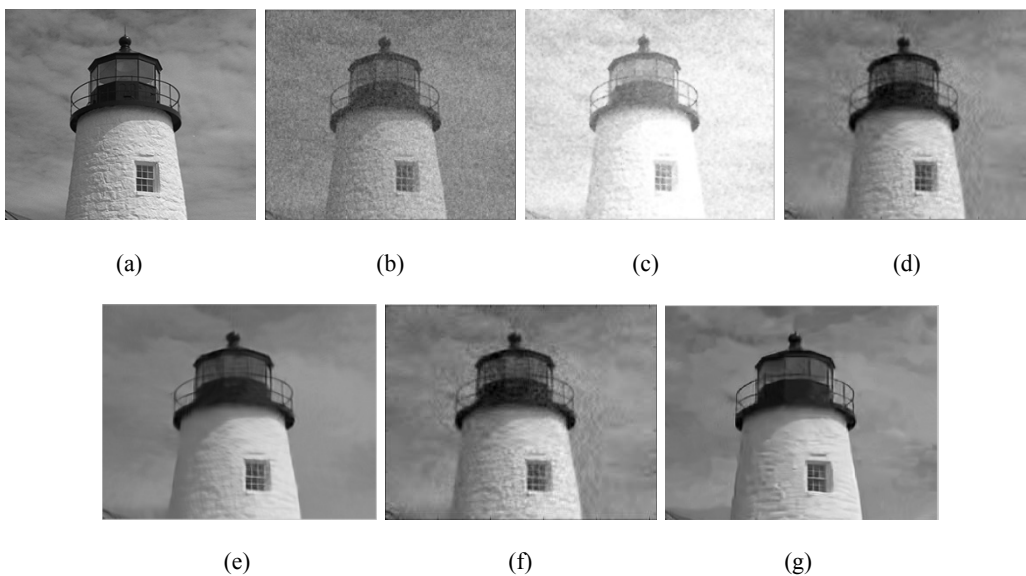


Fig. 6: The denoised images results of tower by different schemes, (a) noisy-free, (b) noisy with $\sigma = 20$, (c-g) are denoised images by using: by contourlet soft, scale mixture using WT, sparse 3D transformation, normal shrink and the suggested algorithm, respectively

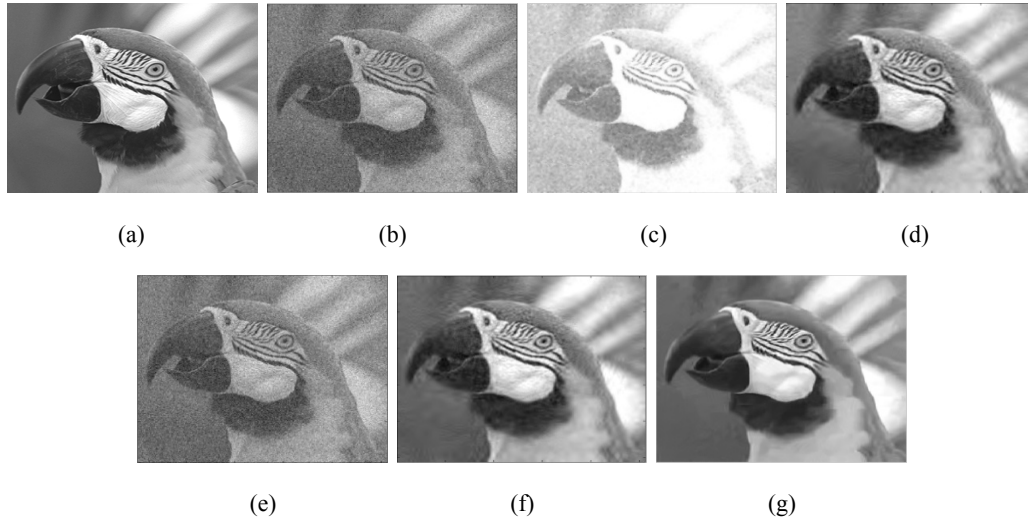


Fig. 7: The denoised images results of parrot by different schemes, (a) noisy-free, (b) noisy with $\sigma = 20$, (c-g) are denoised images by using: by contourlet soft, scale mixture using WT, sparse 3D transformation, normal shrink and the proposed WBD-PCA methods, respectively

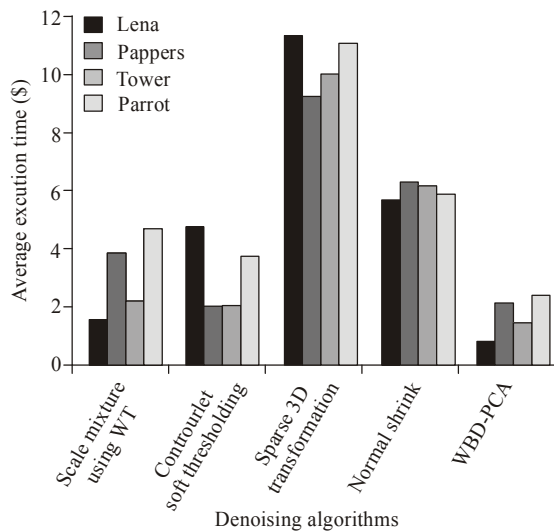


Fig. 8: The average execution time of standard images in (seconds) using different standard algorithms

Figure 8 shows the average execution time in (Seconds) for different standard images (Lena, Peppers, Tower and Parrot) using various standard algorithms. The main goal in this particular point is to find the trade-off between speed and high performance of the algorithm. The average execution time by using WBD-PCA exhibits the shortest time for all images especially for Lena and Tower. It is because second generation wavelet transformation with lifting approach uses perfect reconstruction property and we perform the inverse wavelet by reversing the steps and the processes and apply the interchanging procedure to the mathematical operations in the wavelet domain. On the other hand, Sparse 3D transformation is considered as the slowest algorithm; it took around 11 sec to execute

the algorithm. The reason behind the slow performance of Sparse 3D transformation is resulted because of the large number of logic processes such as additions and multiplications to build the algorithm's structure. Other techniques showed acceptable execution time where the slowest time was 6 sec in Peppers image using Normal shrink, while the fastest was less than 2 sec in Lena image using scale mixture with wavelet transformation.

In short, although the experiments contain images that are rich with complicated textures, the proposed technique outperformed the state-of-the-art denoising algorithms in terms of execution time and it is considered as the fastest algorithm with less than 1 sec. The experiment was conducted in our study using windows 8-based personal computer with (i7) 3.30-GHz CPU processor and 8 GB RAM.

CONCLUSION AND RECOMMENDATIONS

In this study, denoising different standard images were successfully obtained through the semi-soft thresholding of second wavelet transformation (the lifting scheme) combined with principle component analysis, the most beneficial technique in dimensional reduction and denoising approaches. The use of second generation wavelet transformation in our study is quite vital because it has not linked for translation and dilatation processes of the similar wavelet function as it is in the conventional wavelet and the same manner to the scaling functions. In addition, PCA afforded the strength to the algorithm by reducing the dimensionality. Cycle spinning was used in this algorithm to improve the quality of the denoised images in high frequency components such as the edges and other fine image details. The execution time was taken

in our consideration as well. It proves that Sparse 3D transformation is the slowest algorithm, it is because the complex structure of the functions in the algorithm.

The benchmark images that are used in this study were different in texture and structure details, those images were (Lena, Peppers, Parrot and Tower) with size of 256×256. Second generation WBD-PCA denoising algorithm yields smoother results than the state-of-the-art denoising algorithms and it performs well for stationary noise because it tends to treat the appearance variation across viewpoints due to occlusion or reflectivity as noise, it is the consequence of wavelet transformation. Moreover, the usage of PCA drives the target images to be more flexible to preserve these variations and PCA method has the merit among other techniques when it comes to stationary and non-stationary noise. Moreover, from the experimental results we can notice that the proposed algorithm has the best quality in subjective mode from PSNR and SSIM and objectively by the visual perspective to the denoised image. In contrast, the Contourlet soft thresholding has the worst quality among the rest algorithms, even though it has an acceptable result in PSNR and SSIM.

In the future research, we are interested in more principled methods using Markov random field and block matching 3D techniques in order to outline global depth map probability and to combine the multiple denoising processes to achieve more precise results and simple design of the algorithm to reduce the computational complexity. In particular, by using these techniques, we will ensure the sharp edges and very small details in the noisy images will not be ignored by the threshold during the separation process of the pure coefficients from the noisy ones.

REFERENCES

- Abry, P., R. Baraniuk, P. Flandrin, R. Riedi and D. Veitch, 2002. The multiscale nature of network traffic: Discovery, analysis and modeling. *IEEE Signal Proc. Mag.*, 19(3): 28-46.
- Asem, K., A. Ramli, S. Al-Haddad and S. Hashim, 2014. Additive and multiplicative noise removal based on adaptive wavelet transformation using cycle spinning. *Am. J Appl. Sci.*, 11 (2): 316-328.
- Bakshi, B., 1999. Multiscale analysis and modeling using wavelets. *J. Chemometr.*, 13(4): 415-434.
- Chan, T.F. and J. Shen, 2005. *Image Processing and Analysis: Variational, PDE, Wavelet and Stochastic Methods*. Society for Industrial and Applied Mathematics, Philadelphia.
- Donoho, D. and I. Johnstone, 1998. Minimax estimation via wavelet shrinkage. *Ann. Stat.*, 26: 879-921.
- Donoho, D.L., I.M. Johnstone, G. Kerkycharian and D. Picard 1995. Wavelet shrinkage: Asymptopia? *J. Roy. Stat. Soc. B Met.*, 57: 301-369.
- Goldstein, D.E., O.V. Vasilyev, A.A. Wray and R.S. Rogallo, 2000. Evaluation of the use of second generation wavelets in the coherent vortex simulation approach. *Proceedings of the Summer Program Center for Turbulence Research*, pp: 293-304.
- Gruber, P., F.J. Theis, K. Stadlthanner and E.W. Lang, 2004. Denoising using local ICA and kernel-PCA. *Proceedings IEEE International Joint Conference on Neural Networks*, 3: 2071-2076.
- Gupta, V., C. Vikas, C. Chan, C. Poh, T.H. Chow, T.C. Meng and N.B. Koon, 2008. Computerized automation of wavelet based denoising method to reduce speckle noise in OCT images. *Proceeding of 5th International Conference on Information Technology and Applications in Biomedicine (ITAB, 2008)*, pp: 120-123.
- Hesamoddin, J., S. Hamid and H. Gholam Ali, 2005. Noise suppression of fMRI time-series in wavelet domain. *Proceedings of the 7th IASTED International Conference on Signal and Image Processing (SIP, 2005)*, pp: 136-138.
- Hyvarinen, A., J. Karhunen and E. Oja, 2011. *Independent Component Analysis*. John Wiley and Sons Inc., New York.
- Jolliffe, I.T., 2004. *Principal Component Analysis*. Springer Science+Business Media, Inc., New York.
- Liò, P., A.T. Lawniczak, S. Xie and J. Xu, 2008. Wavelet-domain statistics of packet switching networks near traffic congestion. In: Liò, P. *et al.* (Eds.), *BIOWIRE 2007*. LNCS 5151, Springer Verlag, Berlin, Heidelberg, pp: 268-279.
- Mohsen, G., 2004. Adaptive fractal and wavelet image denoising. Ph.D. Thesis, the University of Waterloo.
- Muresan, D.D. and T.W. Parks, 2003. Adaptive principal components and image denoising. *Proceedings of International Conference on Image Processing*, 1: I101-I104.
- Percival, D.P. and A.T. Walden, 2000. *Wavelet Methods for Time Series Analysis*. Cambridge University Press, New York.
- Raanan, F., 2009. A Brief Introduction to First-and Second-generation Wavelets. An Auxiliary Material for the ACM SIGGRAPH Paper: Edge-Avoiding Wavelets and their Applications.
- Starck, J.L., F. Murtagh and A. Bijaoui, 1998. *Image Processing and Data Analysis: The Multiscale Approach*. Cambridge University Press, Cambridge.
- Suganthi, M. and P. Ramamoorthy, 2012. Principal component analysis based feature extraction, morphological edge detection and localization for fast iris recognition. *J. Comput. Sci.*, 8: 1428-1433.

- Wang, Z., A.C. Bovik, H.R. Sheikh and E.P. Simoncelli, 2004. Image quality assessment: From error visibility to structural similarity. *IEEE T. Image Process.*, 13(4): 600-612.
- Weeks, M., 2006. *Digital Signal Processing Using MATLAB and Wavelets*. Infinity Science Press, 25.
- Wink, A.M. and J.B. Roerdink, 2004. Denoising functional MR images: A comparison of wavelet denoising and Gaussian smoothing. *IEEE T. Med. Imaging*, 23(3): 374-387.
- Yasmin, M., M. Sharif, S. Masood, M. Raza and S. Mohsin, 2012. Brain image enhancement-a survey. *World Appl. Sci. J.*, 17: 1192-1204.